

An adaptive cubic regularization method for computing extreme eigenvalues of tensors

Jingya Chang* and Zhi Zhu†

Abstract. In this paper, we compute the H- and Z-eigenvalues of even order symmetric tensors by using the adaptive cubic regularization algorithm. First, the equation of eigenvalues of the tensor is represented by a spherically constrained optimization problem. Owing to the nice geometry of the spherical constraint, we minimize the objective function and preserve the constraint in an alternating way. The objective function of our optimization model is approximated by a cubic function with a tunable parameter, which is solved inexactly to obtain a trial step. Then the Cayley transform is applied to the trial step. Based on the ratio of actual and predicted reductions, a parameter is regulated to make sure that the cubic function is a good estimation of the original objective function. Finally we obtain our adaptive cubic regularization algorithm for computing an eigenvalue of a tensor (ACRCET). Furthermore, we prove that the sequence of iterations generated by ACRCET converges to an eigenvalue of a given tensor globally. In order to improve the computational efficiency, we propose a fast computing skill for $\mathcal{T}\mathbf{x}^{r-2}$ which is the matrix-valued product of a hypergraph related tensor \mathcal{T} and a vector \mathbf{x} . Numerical experiments illustrate that the fast computing skill for $\mathcal{T}\mathbf{x}^{r-2}$ is efficient and our ACRCET is effective when computing eigenvalues of even order symmetric tensors.

Keywords. higher-order tensor, tensor eigenvalue, cubic regularization algorithm, spherically constrained optimization

Mathematics Subject Classification (2020). 15A18, 15A69, 90C30, 90C26

1 Introduction

Eigenvalues of tensors were proposed by Qi [22] and Lim [19] respectively in 2005. From then on, eigenvalues and eigenvectors of tensors have been widely used in science and engineering, such as medical imaging, image processing and spectral graph theory. For example, in magnetic resonance imaging, the

*School of Mathematics and Statistics, Guangdong University of Technology (jychang@gdut.edu.cn). This author's work was supported by the National Natural Science Foundation of China (grant No. 11901118 and 62073087).

†School of Mathematics and Statistics, Guangdong University of Technology (zhzhixixi@163.com).

Z-eigenvectors of the major Z-eigenvalues of an even order tensor express the orientations of crossing nerve fibers in white matter of human brain [7]. The limiting probability distribution vector of a higher-order Markov chain is a Z-eigenvector of a transition probability tensor, and the corresponding eigenvalue is 1 [18]. The Z-eigenvalues of adjacency tensors of even-uniform hypergraphs also have important applications in spectral hypergraph theory [17].

In recent years, the computation of eigenvalues of tensors has been studied by many scholars and different kinds of methods have been proposed. For nonnegative tensors, Ng and Qi [21] extended the method of Collatz (1942) for calculating the spectral radius of an irreducible nonnegative matrix to the calculation of the largest eigenvalue of a nonnegative tensor. A homotopy method was proposed to compute the largest eigenvalues of irreducible nonnegative tensors in [5]. Kuo et al. gave a homotopy continuation method for the computation of nonnegative Z-/H-eigenpairs of nonnegative tensors [16]. Kolda and Mayo [14] proposed a shifted power method to compute Z-eigenpairs of symmetric tensors. Later, they developed an adaptive shifted power method for computing generalized tensor Z-eigenpairs [15]. A shifted inverse power method was introduced in [25] for computing Z-eigenvalues of tensors. Han [12] introduced two unconstrained minimization models to compute the Z-, H-, or D-eigenvalues of even order symmetric tensors.

For computing all eigenvalues of a tensor, Cui et al. [10] used the Jacobian semidefinite relaxations in polynomial optimization to calculate the eigenvalues of a tensor sequentially from the largest one to the smallest one. Chen et al. [6] gave two homotopy continuation type algorithms which can find all equivalent classes of isolated generalized eigenpairs if executed properly. For large scale tensors, Chen et al. [8] introduced an algorithm for computing extreme eigenvalues of large scale Hankel tensors by using the fast Fourier transform. Chang et al. [4] proposed a limited memory BFGS quasi-Newton algorithm for computing eigenvalues of large scale sparse tensors related with a hypergraph.

The cubic estimation model was first introduced in [11] for finding an improved Newton step. Later, the convergence property and numerical performance of the cubic regularization method were broadly studied [1,20,26]. Specifically, some smart worst-case global iteration complexity bounds were established in [2]. The cubic regularization method provides another option beyond trust region and line search methods for unconstrained optimization problems. In this paper, we generalize the cubic regularization method from unconstrained optimization to spherically constrained optimization.

For even order symmetric tensors, we convert the tensor eigenvalue problems to a spherically constrained minimization problem equivalently. To solve this orthogonally constrained model, first we surrogate the objective function by a third order model with an approximated Hessian and find the minimal point of the third order approximation imprecisely at each iteration. Next we push the minimal point onto the the unit sphere by Cayley transform to keep the iteration point feasible. In this step, we use a curvilinear line search so that the objective function value has an appropriate decrease. The approximation function contains a parameter which is adjusted during the iterative process

to insure a good estimation. In terms of eigenvalue problem of tensors arising from a hypergraph, we propose a fast computation algorithm for the repeatedly occurred operation $\mathcal{T}\mathbf{x}^{r-2}$, which is the product of a vector and a tensor arising from a hypergraph. Moreover, we analyze the convergence property of the iterative sequence and prove that the iteration points converge to an eigenvalue of the tensor. We perform numerical experiments and compare our method with PM [14, 15], ACSA [8] and HUOA [12] for computing eigenvalues of even order symmetric tensors.

The outline of this paper is drawn as follows. Basic knowledge about tensors and tensor eigenvalues is given in Section 2. In Section 3, we introduce our algorithm for computing eigenvalues and eigenvectors of an even order symmetric tensor. In Section 4, we demonstrate the global convergence property of our method. In Section 5, we show the fast computation technique for $\mathcal{T}\mathbf{x}^{r-2}$. Numerical experiments on small and medium scale tensors are given in Section 6. Finally, we give some concluding remarks in Section 7.

2 Preliminary

We use boldface Euler script letters such as \mathcal{A} to represent tensors. A matrix is named with a capital letter, while a lower case bold letter is used for a vector and a lower case letter for a scalar. Denote $\mathbb{R}^{[r,n]}$ as the space of r th order n -dimensional real tensors, $\mathbb{R}^{m \times n}$ as the space of real matrices with m rows and n columns, and \mathbb{R}^n as the space of n -dimensional real vectors, where r , m and n are positive integers. Before going to the main results, we introduce the concepts related to tensors.

A tensor $\mathcal{A} \in \mathbb{R}^{[r,n]}$ has n^r entries:

$$\{a_{i_1 i_2 \dots i_r}\}$$

for $i_j \in \{1, 2, \dots, n\}$ and $j \in \{1, 2, \dots, r\}$. A tensor $\mathcal{A} \in \mathbb{R}^{[r,n]}$ is a symmetric tensor if the value of $a_{i_1 i_2 \dots i_r}$ is invariable under any permutation of its indices. An identity tensor $\mathcal{I} \in \mathbb{R}^{[r,n]}$ is a tensor whose diagonal entries are all one and other off-diagonal entries are zero.

For a vector $\mathbf{x} \in \mathbb{R}^n$, we define a scalar $\mathcal{A}\mathbf{x}^r \in \mathbb{R}$,

$$\mathcal{A}\mathbf{x}^r = \sum_{i_1, \dots, i_r=1}^n a_{i_1 i_2 i_3 \dots i_r} x_{i_1} x_{i_2} x_{i_3} \dots x_{i_r},$$

a vector $\mathcal{A}\mathbf{x}^{r-1} \in \mathbb{R}^n$,

$$(\mathcal{A}\mathbf{x}^{r-1})_p = \sum_{i_2, \dots, i_r=1}^n a_{p i_2 i_3 \dots i_r} x_{i_2} x_{i_3} \dots x_{i_r}, \forall p \in \{1, 2, \dots, n\},$$

and a matrix $\mathcal{A}\mathbf{x}^{r-2} \in \mathbb{R}^{n \times n}$,

$$(\mathcal{A}\mathbf{x}^{r-2})_{pq} = \sum_{i_3, \dots, i_r=1}^n a_{p q i_3 \dots i_r} x_{i_3} \dots x_{i_r}, \forall p, q \in \{1, 2, \dots, n\}.$$

Definition 2.1 (H-eigenvalue and H-eigenvector [22]). *If there exist a $\lambda \in \mathbb{R}$ and a nonzero vector $\mathbf{x} \in \mathbb{R}^n$ such that*

$$\mathcal{A}\mathbf{x}^{r-1} = \lambda\mathbf{x}^{[r-1]}, \quad (1)$$

then λ is called an H-eigenvalue of \mathcal{A} and \mathbf{x} is its associated H-eigenvector, where $\mathbf{x}^{[r-1]} =: (x_1^{r-1}, x_2^{r-2}, \dots, x_n^{r-1})^T$.

Definition 2.2 (Z-eigenvalue and Z-eigenvector [22]). *Suppose that (λ, \mathbf{x}) is a solution pair of the following system*

$$\mathcal{A}\mathbf{x}^{r-1} = \lambda\mathbf{x} \quad \text{and} \quad \mathbf{x}^T\mathbf{x} = 1, \quad (2)$$

then λ is called a Z-eigenvalue of \mathcal{A} and \mathbf{x} is its associated Z-eigenvector.

3 Computation of eigenvalues of tensors

In this section, we demonstrate our method for computing H- and Z-eigenvalues of an even order symmetric tensor.

3.1 The equivalent optimization model of tensor eigenvalue problems

The equation systems in (1) and (2) can be changed to a spherically constrained optimization problem [4]. Consider the following optimization problem

$$\min f(\mathbf{x}) := \frac{\mathcal{A}\mathbf{x}^r}{\mathcal{B}\mathbf{x}^r} \quad \text{s.t.} \quad \mathbf{x} \in \mathbb{S}^{n-1}, \quad (3)$$

where \mathcal{A} and \mathcal{B} are symmetric tensors, the set $\mathbb{S}^{n-1} := \{\mathbf{x} \in \mathbb{R}^n : \mathbf{x}^T\mathbf{x} = 1\}$ is a unit spherical surface. The gradient of $f(\mathbf{x})$ is

$$\nabla f(\mathbf{x}) = \frac{r}{\mathcal{B}\mathbf{x}^r} \left(\mathcal{A}\mathbf{x}^{r-1} - \frac{\mathcal{A}\mathbf{x}^r}{\mathcal{B}\mathbf{x}^r} \mathcal{B}\mathbf{x}^{r-1} \right). \quad (4)$$

When $\nabla f(\mathbf{x}) = 0$, we have $\mathcal{A}\mathbf{x}^{r-1} = \frac{\mathcal{A}\mathbf{x}^r}{\mathcal{B}\mathbf{x}^r} \mathcal{B}\mathbf{x}^{r-1}$. In [12], it is shown that when $\mathcal{B} = \mathcal{I}$,

$$\mathcal{B}\mathbf{x}^r = \|\mathbf{x}\|_r^r, \quad \mathcal{B}\mathbf{x}^{r-1} = \mathbf{x}^{[r-1]}.$$

When r is even and $\mathcal{B} = I^{\frac{r}{2}}$,

$$\mathcal{B}\mathbf{x}^r = \|\mathbf{x}\|_2^r = 1, \quad \mathcal{B}\mathbf{x}^{r-1} = \|\mathbf{x}\|_2^{r-2} \mathbf{x} = \mathbf{x}.$$

Thus for even order tensors, $f(\mathbf{x}) = \mathcal{A}\mathbf{x}^r / \mathcal{B}\mathbf{x}^r$ is the H-eigenvalue or Z-eigenvalue of \mathcal{A} when $\mathcal{B} = \mathcal{I}$ or $\mathcal{B} = I^{\frac{r}{2}}$ respectively at the stationary point \mathbf{x} , and \mathbf{x} is the corresponding eigenvector. On the other hand, we can verify that when $\mathcal{B} = \mathcal{I}$ or $\mathcal{B} = I^{\frac{r}{2}}$ and \mathbf{x} is the H- or Z-eigenvector of \mathcal{A} , the eigenvector \mathbf{x} is the stationary point with the eigenvalue being $\frac{\mathcal{A}\mathbf{x}^r}{\mathcal{B}\mathbf{x}^r}$.

Therefore, the eigenvalue problems are equivalently transformed to the question of finding the stationary point of the objective function in (3) on the unit sphere.

3.2 Adaptive cubic regularization method

In this section, we design an adaptive cubic regularization method for solving the spherically constrained optimization problem (3). By calculating, we get the Hessian $\nabla^2 f(\mathbf{x})$ of $f(\mathbf{x})$ as follows

$$\nabla^2 f(\mathbf{x}_k) = \frac{r(r-1)}{\mathcal{B}\mathbf{x}^r} \mathcal{A}\mathbf{x}^{r-2} - \frac{r^2}{(\mathcal{B}\mathbf{x}^r)^2} (\mathcal{A}\mathbf{x}^{r-1} \odot \mathcal{B}\mathbf{x}^{r-1}) \quad (5)$$

$$- \frac{r(r-1)\mathcal{A}\mathbf{x}^r}{(\mathcal{B}\mathbf{x}^r)^2} \mathcal{B}\mathbf{x}^{r-2} + \frac{r^2 \mathcal{A}\mathbf{x}^r}{(\mathcal{B}\mathbf{x}^r)^3} (\mathcal{B}\mathbf{x}^{r-1} \odot \mathcal{B}\mathbf{x}^{r-1}). \quad (6)$$

The symbol \odot refers to the operation $\mathbf{a} \odot \mathbf{b} = \mathbf{a}\mathbf{b}^T + \mathbf{b}\mathbf{a}^T$ for two vectors \mathbf{a} and \mathbf{b} . Clearly, the function $f(\mathbf{x})$ is three times continuously differentiable.

Lemma 3.1. *Since $f(\mathbf{x})$ is three times continuously differentiable on the compact set \mathbb{S}^{n-1} , there exists a constant M such that*

$$\|f(\mathbf{x})\| \leq M, \|\nabla f(\mathbf{x})\| \leq M, \|\nabla^2 f(\mathbf{x})\| \leq M. \quad (7)$$

Also $\nabla^2 f(\mathbf{x})$ is globally Lipschitz continuous, which means there exists a constant $L > 0$ such that

$$\|\nabla^2 f(\mathbf{x}) - \nabla^2 f(\tilde{\mathbf{x}})\| \leq L\|\mathbf{x} - \tilde{\mathbf{x}}\| \quad (8)$$

for any \mathbf{x} and $\tilde{\mathbf{x}} \in \mathbb{S}^{n-1}$.

Denote $f_k = f(\mathbf{x}_k)$, $\mathbf{g}_k = \nabla f(\mathbf{x}_k)$ and $H_k = \nabla^2 f(\mathbf{x}_k)$. Let \mathbf{p} be a direction pointing from the vector \mathbf{x}_k . By expressing the Taylor expansion of $f(\mathbf{x}_k + \mathbf{p})$ at the point \mathbf{x}_k , we get

$$\begin{aligned} f(\mathbf{x}_k + \mathbf{p}) &= f_k + \mathbf{g}_k^T \mathbf{p} + \frac{1}{2} \mathbf{p}^T H_k \mathbf{p} + \int_0^1 (1-t) \mathbf{p}^T [H(\mathbf{x}_k + t\mathbf{p}) - H(\mathbf{x}_k)] \mathbf{p} dt \\ &\leq f_k + \mathbf{g}_k^T \mathbf{p} + \frac{1}{2} \mathbf{p}^T H_k \mathbf{p} + \frac{1}{6} L \|\mathbf{p}\|_2^3, \end{aligned} \quad (9)$$

in which the inequality is deduced from the Lipschitz property of $\nabla^2 f(\mathbf{x})$. In [1], Cartis et al. introduced a dynamic parameter σ_k instead of $\frac{1}{2}L$ and suggested to use

$$f_k + \mathbf{g}_k^T \mathbf{p} + \frac{1}{2} \mathbf{p}^T H_k \mathbf{p} + \frac{1}{3} \sigma_k \|\mathbf{p}\|_2^3 \quad (10)$$

as the approximation to $f(\mathbf{x}_k + \mathbf{p})$. Since the function f is restricted on the unit spherical surface, we project the Hessian matrix H_k onto the tangent space at \mathbf{x} by the projection matrix $P_k := (I - \mathbf{x}_k \mathbf{x}_k^T)$, and get $B_k := P_k H_k P_k$. The estimation in (10) is further modified by

$$f_k + \mathbf{g}_k^T \mathbf{p} + \frac{1}{2} \mathbf{p}^T B_k \mathbf{p} + \frac{1}{3} \sigma_k \|\mathbf{p}\|_2^3. \quad (11)$$

Thus in each iteration, we solve the subproblem

$$\min m_k(\mathbf{p}) := f_k + \mathbf{g}_k^T \mathbf{p} + \frac{1}{2} \mathbf{p}^T B_k \mathbf{p} + \frac{1}{3} \sigma_k \|\mathbf{p}\|_2^3 \quad (12)$$

to find a descent direction \mathbf{p}_k .

In order to improve the computing efficiency, the subproblem (12) is solved inexactly. Denote \mathbf{p}_k^C as the Cauchy point of $m_k(\mathbf{p})$, that means

$$\mathbf{p}_k^C = -\tau_k^C \mathbf{g}_k \quad \text{and} \quad \tau_k^C = \arg \min_{\tau \in \mathbb{R}^+} m_k(-\tau \mathbf{g}_k).$$

A vector \mathbf{p}_k is chosen once it satisfies

$$m_k(\mathbf{p}_k) \leq m_k(\mathbf{p}_k^C).$$

The parameter σ_k is updated adaptively in light of the ratio of actual reduction to predicted reduction, details of which will be explained in the next subsection.

3.3 Cayley transform, curvilinear search and parameter tuning

Based on the direction \mathbf{p}_k getting from (12), we employ the Cayley transform [3] to generate an orthogonal matrix and obtain a new feasible point. At the same time, we perform a curvilinear search on \mathbb{S}^{n-1} to guarantee that the objective function value decrease. The parameter σ is tuned according to the accuracy of the estimation term.

Define a skew-symmetric matrix $W_k(\alpha) \in \mathbb{R}^{n \times n}$ as

$$W_k(\alpha) = \frac{\alpha}{2}(\mathbf{x}_k \mathbf{p}_k^T - \mathbf{p}_k \mathbf{x}_k^T), \quad (13)$$

where $\alpha > 0$ is a parameter. Then $(I + W_k(\alpha))$ is invertible, and the Cayley transform produces an orthogonal matrix

$$Q_k(\alpha) = (I + W_k(\alpha))^{-1}(I - W_k(\alpha)). \quad (14)$$

For $\mathbf{x}_k \in \mathbb{S}^{n-1}$, the vector

$$\mathbf{x}_k^+(\alpha) := Q_k(\alpha) \mathbf{x}_k \quad (15)$$

also belongs to \mathbb{S}^{n-1} . Substituting (13) and (14) into (15), the vector $\mathbf{x}_k^+(\alpha)$ can be computed through the following formula [4]

$$\mathbf{x}_k^+(\alpha) = \frac{[(2 - \alpha \mathbf{p}_k^T \mathbf{x}_k)^2 - \alpha^2 \|\mathbf{p}_k\|^2] \mathbf{x}_k + 4\alpha \mathbf{p}_k}{4 + \alpha^2 \|\mathbf{p}_k\|^2 - \alpha^2 (\mathbf{p}_k^T \mathbf{x}_k)^2}. \quad (16)$$

Next, a curvilinear search process by (16) is implemented to determine the step size α . Define the ratio of actual reduction in f to predicted reduction in m_k as

$$\rho_k := \frac{f(\mathbf{x}_k) - f(\mathbf{x}_k^+(\alpha))}{m_k(0) - m_k(\alpha \mathbf{p}_k)}. \quad (17)$$

Take $\alpha = 1$ initially. If ρ_k is greater than or equal to a positive constant η_1 ($\eta_1 \in (0, 1)$), the step size α is accepted and the new iterate $\mathbf{x}_{k+1} = \mathbf{x}_k^+(\alpha)$.

Otherwise, we decrease the step size α and repeat until $\rho_k \geq \eta_1$. If $\alpha_k = 1$ and ρ_k is greater than or equal to a given number, we regard m_k as a very successful estimation of the original function f and decrease the value of σ in the next step. If not, the value of σ is increased in the next step. We describe the updating scheme in detail in Algorithm 1.

4 Convergence analysis

In this section, we analyze the convergence property of the ACRRET method. We show that the gradient norm $\|\mathbf{g}_k\|$ generated by Algorithm 1 converges to 0 globally. Thus we obtain the stationary point which is an eigenvector of the given tensor, and its function value is the eigenvalue.

First we explain that the step size α_k is bounded away from zero in our iteration process. Then we prove

$$\liminf_{k \rightarrow \infty} \|\mathbf{g}_k\| = 0 \quad (18)$$

by contradiction. Based on (18), we further obtain the convergence result of $\{\mathbf{g}_k\}$.

Cartis et al. [1] gave a lower bound on the decrease in f predicted from the cubic model $m_k(\mathbf{p}_k)$ and a bound on $\|\mathbf{p}_k\|$. These two conclusions, which are useful in the convergence analysis, also hold for our algorithm.

Lemma 4.1 ([1]). *Suppose that the step \mathbf{p}_k satisfies $m_k(\mathbf{p}_k) \leq m_k(\mathbf{p}_k^C)$. Then for all $k \geq 0$, we have*

$$f(\mathbf{x}_k) - m_k(\mathbf{p}_k) \geq \frac{\|\mathbf{g}_k\|}{6\sqrt{2}} \min \left[\frac{\|\mathbf{g}_k\|}{1 + \|B_k\|}, \frac{1}{2} \sqrt{\frac{\|\mathbf{g}_k\|}{\sigma_k}} \right] \quad (19)$$

and

$$\|\mathbf{p}_k\| \leq \frac{3}{\sigma_k} \max (M, \sqrt{\sigma_k \|\mathbf{g}_k\|}). \quad (20)$$

Now we prove that α_k is bounded above 0.

Lemma 4.2. *For the step size α_k generated by Algorithm 1, it holds that*

$$\liminf_{k \rightarrow \infty} \alpha_k > 0.$$

Proof. We prove the conclusion by contradiction. Suppose that a subsequence of $\{\alpha_{k_i}\}$ tends to 0. By the rule of backtracking search in Algorithm 1, we have

$$\frac{f_{k_i} - f(x_{k_i}^+(\gamma_1^{-1}\alpha_{k_i}))}{f_{k_i} - m_{k_i}(\gamma_1^{-1}\alpha_{k_i}\mathbf{p}_{k_i})} < \eta_1. \quad (21)$$

Since the objective function is zero-order homogeneous, then

$$\mathbf{g}_k^T \mathbf{x}_k = 0. \quad (22)$$

Algorithm 1 An adaptive cubic regularization algorithm for computing an eigenvalue of a tensor.(ACRCET)

- 1: Set $\mathcal{B} = \mathcal{I}$ and $\mathcal{B} = I^{\frac{r}{2}}$ when calculating an H-eigenvalue and a Z-eigenvalue of a tensor \mathcal{A} respectively.
- 2: Set parameters $\gamma_3 \geq \gamma_2 > 1 > \gamma_1 > 0$, $1 > \eta_2 \geq \eta_1 > 0$, and $\sigma_0 > 0$ for $k = 0, 1, \dots$ until convergence. Choose an initial point $\mathbf{x}_0 \in \mathbb{S}^{n-1}$ and set $k \leftarrow 0$.
- 3: **while** $\nabla f(\mathbf{x}_k) \neq 0$ **do**
- 4: Calculate $\mathcal{A}\mathbf{x}^r$, $\mathcal{B}\mathbf{x}^r$, $\mathcal{A}\mathbf{x}^{r-1}$, $\mathcal{B}\mathbf{x}^{r-1}$, $\mathcal{A}\mathbf{x}^{r-2}$, and $\mathcal{B}\mathbf{x}^{r-2}$.
- 5: Solve the subproblem:

$$\min_{\mathbf{p}} f_k + \mathbf{g}_k^T \mathbf{p} + \frac{1}{2} \mathbf{p}^T B_k \mathbf{p} + \frac{1}{3} \sigma_k \|\mathbf{p}\|^3,$$

for a trial step \mathbf{p}_k satisfying

$$m_k(\mathbf{p}_k) \leq m_k(\mathbf{p}_k^C)$$

where the Cauchy point

$$\mathbf{p}_k^C = -\tau_k^C \mathbf{g}_k \text{ and } \tau_k^C = \arg \min_{\tau \in \mathbb{R}^+} m_k(-\tau \mathbf{g}_k).$$

- 6: Compute $f(\mathbf{x}_k^+(\alpha))$ by (16) and (3). Find the smallest nonnegative integer j such that the step size $\alpha = \gamma_1^j$ satisfies

$$\rho_k = \frac{f(\mathbf{x}_k) - f(\mathbf{x}_k^+(\alpha))}{m_k(0) - m_k(\alpha \mathbf{p}_k)} \geq \eta_1.$$

- 7: Set $\alpha_k = \gamma_1^j$ and $\mathbf{x}_{k+1} = \mathbf{x}_k^+(\alpha_k)$.
- 8: If $\alpha_k = 1$, set

$$\sigma_{k+1} \in \begin{cases} [0, \sigma_k] & \text{if } \rho_k > \eta_2 & \text{[very successful iteration],} \\ [\sigma_k, \gamma_2 \sigma_k] & \text{if } \eta_1 \leq \rho_k \leq \eta_2 & \text{[successful iteration],} \end{cases}$$

else

$$\sigma_{k+1} \in [\gamma_2 \sigma_k, \gamma_3 \sigma_k] \quad \text{[unsuccessful iteration].}$$

- 9: Set $k \leftarrow k + 1$
 - 10: **end while**
-

It can be calculated from (16) that

$$\mathbf{x}_k'^+(0) = -\mathbf{x}_k^T \mathbf{p}_k \mathbf{x}_k + \mathbf{p}_k. \quad (23)$$

By (22) and (23) we obtain

$$\left. \frac{df(\mathbf{x}_k^+(\alpha))}{d\alpha} \right|_{\alpha=0} = \nabla f(\mathbf{x}_k^+(0))^T \mathbf{x}_k'^+(0) = \nabla f(\mathbf{x}_k)^T (-\mathbf{x}_k^T \mathbf{p}_k \mathbf{x}_k + \mathbf{p}_k) = \mathbf{g}_k^T \mathbf{p}_k$$

and

$$\left. \frac{d^2 f(\mathbf{x}_k^+(\alpha))}{d\alpha^2} \right|_{\alpha=0} = \mathbf{p}_k^T B_k \mathbf{p}_k.$$

Thus by substituting the Taylor series expansion of $f(x_{k_i}^+(\gamma_1^{-1} \alpha_{k_i}))$ around the point $\alpha = 0$ and the expression of $m_{k_i}(\gamma_1^{-1} \alpha_{k_i} \mathbf{p}_{k_i})$ into (21), we have

$$\begin{aligned} & \eta_1 (-\gamma_1^{-1} \alpha_{k_i} \mathbf{g}_{k_i}^T \mathbf{p}_{k_i} - \frac{1}{2} (\gamma_1^{-1} \alpha_{k_i})^2 \mathbf{p}_{k_i}^T B_{k_i} \mathbf{p}_{k_i} - \frac{1}{3} \sigma_k \|\gamma_1^{-1} \alpha_{k_i} \mathbf{p}_{k_i}\|^3) \\ & + \gamma_1^{-1} \alpha_{k_i} \mathbf{g}_{k_i}^T \mathbf{p}_{k_i} + \frac{1}{2} (\gamma_1^{-1} \alpha_{k_i})^2 \mathbf{p}_{k_i}^T B_{k_i} \mathbf{p}_{k_i} + o\left(\frac{\alpha_{k_i}^2}{\gamma_1^2}\right) > 0. \end{aligned}$$

The above inequality is equivalent to

$$(1 - \eta_1) \mathbf{g}_{k_i}^T \mathbf{p}_{k_i} + \frac{\alpha_{k_i}}{2\gamma_1} ((1 - \eta_1) \mathbf{p}_{k_i}^T B_{k_i} \mathbf{p}_{k_i}) - \frac{\alpha_{k_i}^2 \eta_1 \sigma_k}{3\gamma_1^2} \|\mathbf{p}_{k_i}\|^3 + o\left(\frac{\alpha_{k_i}}{\gamma_1}\right) > 0. \quad (24)$$

Since $\{\mathbf{x}_{k_i}\}$ is on the the unit sphere, there exists a subsequence of $\{\mathbf{x}_{k_i}\}$ that converges to a limit point \tilde{x} . Without confusion, we use $\{\mathbf{x}_{k_i}\}$ to refer to the subsequence whereafter in this proof. Therefore, we have $\mathbf{g}_{k_i} \rightarrow \mathbf{g}_\infty$, $B_{k_i} \rightarrow B_\infty$ and $\mathbf{p}_{k_i} \rightarrow \mathbf{p}_\infty$. By taking $i \rightarrow \infty$, we get $\mathbf{g}_\infty^T \mathbf{p}_\infty \geq 0$ from (24) and the hypothesis that $\alpha_{k_i} \rightarrow 0$. On the other hand, in the iteration process $\mathbf{g}_k^T \mathbf{p}_k \leq 0$. These two inequalities indicate that

$$\mathbf{g}_\infty^T \mathbf{p}_\infty = 0.$$

Thus when i is large enough, from (24) we get

$$\frac{1 - \eta_1}{2} \mathbf{p}_{k_i}^T B_{k_i} \mathbf{p}_{k_i} - \frac{\alpha_{k_i} \eta_1 \sigma_k}{3\gamma_1} \|\mathbf{p}_{k_i}\|^3 > 0. \quad (25)$$

Taking $i \rightarrow \infty$, the above inequality becomes

$$\mathbf{p}_\infty^T B_\infty \mathbf{p}_\infty > 0. \quad (26)$$

Next, we show

$$\mathbf{p}_\infty^T B_\infty \mathbf{p}_\infty < 0 \quad (27)$$

based on (19). In fact

$$f(\mathbf{x}_k) - m_k(\mathbf{p}_k) \geq 0$$

in Lemma 4.1 means that

$$-\mathbf{g}_{k_i}^T \mathbf{p}_{k_i} - \frac{1}{2} \mathbf{p}_{k_i}^T B_{k_i} \mathbf{p}_{k_i} - \frac{1}{3} \sigma_{k_i} \|\mathbf{p}_{k_i}\|^3 \geq 0. \quad (28)$$

By taking $i \rightarrow \infty$, we obtain $\mathbf{p}_\infty^T B_\infty \mathbf{p}_\infty \leq -\frac{2}{3} \sigma_\infty \|\mathbf{p}_\infty\|^3 \leq 0$, which contradicts with the inequality (26).

Hence, $\{\alpha_k\}$ is bounded above 0 and there exists a positive number α_{\min} such that $\alpha_k \geq \alpha_{\min}$ for all k . \square

Next We prove $\liminf_{k \rightarrow \infty} \|\mathbf{g}_k\| = 0$ by reductio ad absurdum. Assume there exists a constant $\epsilon > 0$ such that $\|\mathbf{g}_k\| \geq \epsilon$ for any k . First we illustrate that $\sqrt{\frac{\|\mathbf{g}_k\|}{\sigma_k}}$ is a convergent series in Lemma 4.3. Then we show that the parameter σ_k is monotonically non-increasing when k is large enough in Lemma 4.4. Finally, contradiction emerges on the basis of these two Lemmas.

Lemma 4.3. *Suppose \mathbf{x}_k , \mathbf{g}_k and σ_k are produced from Algorithm 1. Then we have*

$$\sum_{k=1}^{+\infty} \sqrt{\frac{\|\mathbf{g}_k\|}{\sigma_k}} < +\infty \quad (29)$$

and

$$\|\mathbf{p}_k\| \leq 3 \sqrt{\frac{\|\mathbf{g}_k\|}{\sigma_k}} \quad (30)$$

under the assumption $\|\mathbf{g}_k\| \geq \epsilon$.

Proof. From the definition of m_k in (12) we have

$$m_k(\mathbf{p}_k) - f(\mathbf{x}_k) = \mathbf{g}_k^T \mathbf{p}_k + \frac{1}{2} \mathbf{p}_k^T B_k \mathbf{p}_k + \frac{1}{3} \sigma_k \|\mathbf{p}_k\|^3 \quad (31)$$

$$m_k(\alpha \mathbf{p}_k) - f(\mathbf{x}_k) = \alpha \mathbf{g}_k^T \mathbf{p}_k + \frac{1}{2} \alpha^2 \mathbf{p}_k^T B_k \mathbf{p}_k + \frac{1}{3} \sigma_k \alpha^3 \|\mathbf{p}_k\|^3. \quad (32)$$

The process of generating \mathbf{p}_k in Algorithm 1 means that

$$m_k(\mathbf{p}_k) - f(\mathbf{x}_k) \leq m_k(\mathbf{p}_k^C) - f(\mathbf{x}_k) \leq 0.$$

Therefore $\mathbf{g}_k^T \mathbf{p}_k + \frac{1}{2} \mathbf{p}_k^T B_k \mathbf{p}_k \leq 0$ and for any $\alpha_k \in (0, 1]$ we have

$$\alpha_k^3 (\mathbf{g}_k^T \mathbf{p}_k + \frac{1}{2} \mathbf{p}_k^T B_k \mathbf{p}_k) \geq \alpha_k^2 (\mathbf{g}_k^T \mathbf{p}_k + \frac{1}{2} \mathbf{p}_k^T B_k \mathbf{p}_k) \geq \alpha_k \mathbf{g}_k^T \mathbf{p}_k + \frac{1}{2} \alpha_k^2 \mathbf{p}_k^T B_k \mathbf{p}_k.$$

Combining (31) with (32), we get

$$f(\mathbf{x}_k) - m_k(\alpha_k \mathbf{p}_k) \geq \alpha_k^3 (f(\mathbf{x}_k) - m_k(\mathbf{p}_k)).$$

Therefore

$$\begin{aligned}
f(\mathbf{x}_k) - f(\mathbf{x}_{k+1}) &\geq \eta_1 [f(\mathbf{x}_k) - m_k(\alpha_k \mathbf{p}_k)] \geq \alpha_k^3 \eta_1 [f(\mathbf{x}_k) - m_k(\mathbf{p}_k)] \\
&\geq \frac{\alpha_{\min}^3 \eta_1 \|\mathbf{g}_k\|}{6\sqrt{2}} \min \left[\frac{\|\mathbf{g}_k\|}{1 + \|B_k\|}, \frac{1}{2} \sqrt{\frac{\|\mathbf{g}_k\|}{\sigma_k}} \right] \quad (\text{Due to 19 and Lemma 4.2}) \\
&\geq \frac{\alpha_{\min}^3 \eta_1 \epsilon}{6\sqrt{2}} \min \left[\frac{\epsilon}{1 + M}, \frac{1}{2} \sqrt{\frac{\|\mathbf{g}_k\|}{\sigma_k}} \right] \quad (\text{Because } \|\mathbf{g}_k\| \geq \epsilon \text{ and } \|B_k\| \leq M)
\end{aligned} \tag{33}$$

Since $m_k(\mathbf{p}_k) - f(\mathbf{x}_k) \leq 0$, the sequence $\{f(\mathbf{x}_k)\}$ is monotonically decreasing. Moreover $\{f(\mathbf{x}_k)\}$ is bounded below, and therefore it is convergent. Suppose $\lim_{k \rightarrow +\infty} f(\mathbf{x}_k) = f^*$. Hence, when k is large enough $f(\mathbf{x}_k) - f(\mathbf{x}_{k+1})$ tends to zero. Based on (33) we obtain

$$\sqrt{\frac{\|\mathbf{g}_k\|}{\sigma_k}} \rightarrow 0 \quad \text{as } k \rightarrow \infty \tag{34}$$

from the last inequality and

$$\begin{aligned}
\sum_{k=k_0}^{+\infty} [f(\mathbf{x}_k) - f(\mathbf{x}_{k+1})] &= f(\mathbf{x}_{k_0}) - f^* \\
&\geq \sum_{k=k_0}^{+\infty} \frac{\alpha_{\min}^3 \eta_1 \epsilon}{6\sqrt{2}} \min \left[\frac{\epsilon}{1 + M}, \frac{1}{2} \sqrt{\frac{\|\mathbf{g}_k\|}{\sigma_k}} \right].
\end{aligned}$$

Since $f(\mathbf{x}_k)$ is bounded, the conclusion in (29) holds immediately.

Since $\|\mathbf{g}_k\| \geq \epsilon$, then we get $\sqrt{\sigma_k \|\mathbf{g}_k\|} \geq \epsilon \sqrt{\frac{\sigma_k}{\|\mathbf{g}_k\|}} \rightarrow +\infty$ from (34). With the help of (20), the inequality

$$\|\mathbf{p}_k\| \leq 3 \sqrt{\frac{\|\mathbf{g}_k\|}{\sigma_k}} \tag{35}$$

holds for k is large enough. \square

Denote an index set $\mathcal{U} := \{k : \|\mathbf{g}_k\| \geq \epsilon \text{ and } \sqrt{\frac{\|\mathbf{g}_k\|}{\sigma_k}} \rightarrow 0 \text{ as } k \rightarrow \infty\}$. We get the following results about σ_k when $k \in \mathcal{U}$ is large enough.

Lemma 4.4. *When $k \in \mathcal{U}$ and $k \rightarrow \infty$, for each iteration $k \in \mathcal{U}$ that is sufficiently large, we obtain*

$$\sigma_{k+1} \leq \sigma_k. \tag{36}$$

Proof. Let $\alpha = 1$. With the help of Lemma 3.1, it can be deduced from the Taylor expansion of $f(\mathbf{x}_k^+(1))$ at the point \mathbf{x}_k that

$$f(\mathbf{x}_k^+(1)) \leq f_k + \mathbf{g}_k^T(\mathbf{x}_k^+(1) - \mathbf{x}_k) + \frac{M}{2} \|\mathbf{x}_k^+(1) - \mathbf{x}_k\|^2.$$

Then

$$f(\mathbf{x}_k^+(1)) - m_k(\mathbf{p}_k) \leq \mathbf{g}_k^T(\mathbf{x}_k^+(1) - \mathbf{x}_k - \mathbf{p}_k) + \frac{M}{2} (\|\mathbf{x}_k^+(1) - \mathbf{x}_k\|^2 + \|\mathbf{p}_k\|^2) - \frac{\sigma_k}{3} \|\mathbf{p}_k\|^3. \quad (37)$$

From (22) and (16), we obtain

$$|\mathbf{g}_k^T(\mathbf{x}_k^+(1) - \mathbf{x}_k - \mathbf{p}_k)| = |\mathbf{g}_k^T \mathbf{p}_k| \left| \frac{\|\mathbf{p}_k\|^2 - (\mathbf{p}_k^T \mathbf{x}_k)^2}{4 + \|\mathbf{p}_k\|^2 - (\mathbf{p}_k^T \mathbf{x}_k)^2} \right| \leq \frac{|\mathbf{g}_k^T \mathbf{p}_k|}{4} \|\mathbf{p}_k\|^2 \leq \frac{M}{4} \|\mathbf{p}_k\|^3. \quad (38)$$

Because $\mathbf{x}_k^+(\alpha)$ and \mathbf{x}_k belong to \mathbb{S}^{n-1} and $\alpha \in (0, 1]$, by (16) we have

$$\|\mathbf{x}_k^+(\alpha) - \mathbf{x}_k\|^2 = 2 - 2(\mathbf{x}_k^+(\alpha))^T \mathbf{x}_k = \frac{4\alpha^2(\|\mathbf{p}_k\|^2 - (\mathbf{p}_k^T \mathbf{x}_k)^2)}{4 + \alpha^2\|\mathbf{p}_k\|^2 - \alpha^2(\mathbf{p}_k^T \mathbf{x}_k)^2} \leq \|\mathbf{p}_k\|^2. \quad (39)$$

Then we get

$$\|\mathbf{x}_k^+(1) - \mathbf{x}_k\|^2 \leq \|\mathbf{p}_k\|^2. \quad (40)$$

Combining (37), (38) and (40), we have

$$f(\mathbf{x}_k^+(1)) - m_k(\mathbf{p}_k) \leq \frac{M}{4} \|\mathbf{p}_k\|^3 + M \|\mathbf{p}_k\|^2 - \frac{\sigma_k}{3} \|\mathbf{p}_k\|^3.$$

Substituting (35) into the above inequality, we obtain

$$f(\mathbf{x}_k^+(1)) - m_k(\mathbf{p}_k) \leq \left[9M \sqrt{\frac{\|\mathbf{g}_k\|}{\sigma_k}} + \left(\frac{27M}{4} - 9\sigma_k \right) \frac{\|\mathbf{g}_k\|}{\sigma_k} \right] \sqrt{\frac{\|\mathbf{g}_k\|}{\sigma_k}}, \quad (41)$$

for all $k \in \mathcal{U}$ sufficiently large.

On the other hand, since $\|\mathbf{g}_k\| \geq \epsilon$ and $\|B_k\| \leq M$, we have

$$f(\mathbf{x}_k) - m_k(\mathbf{p}_k) \geq \frac{\epsilon}{6\sqrt{2}} \min \left[\frac{\epsilon}{1+M}, \frac{1}{2} \sqrt{\frac{\|\mathbf{g}_k\|}{\sigma_k}} \right], \quad \text{for all } k \in \mathcal{U},$$

from (19). Hence, for all $k \in \mathcal{U}$ sufficiently large, the above inequality means

$$f(\mathbf{x}_k) - m_k(\mathbf{p}_k) \geq \frac{\epsilon}{12\sqrt{2}} \sqrt{\frac{\|\mathbf{g}_k\|}{\sigma_k}}. \quad (42)$$

By the rule of updating σ_k in Algorithm 1, we have

$$\begin{aligned} & k\text{th iteration is very successful} \\ \iff & \rho_k > \eta_2 \text{ and } \alpha_k = 1 \\ \iff & r_k := f(\mathbf{x}_k^+(1)) - f(\mathbf{x}_k) - \eta_2 [m_k(\mathbf{p}_k) - f(\mathbf{x}_k)] < 0. \end{aligned}$$

The formula of r_k can be equivalently expressed as

$$r_k = f(\mathbf{x}_k^+(1)) - m_k(\mathbf{p}_k) + (1 - \eta_2)[m_k(\mathbf{p}_k) - f(\mathbf{x}_k)]. \quad (43)$$

Combining (41) (42) with (43), we obtain

$$r_k \leq \sqrt{\frac{\|\mathbf{g}_k\|}{\sigma_k}} \left[9M \sqrt{\frac{\|\mathbf{g}_k\|}{\sigma_k}} + \left(\frac{27M}{4} - 9\sigma_k \right) \frac{\|\mathbf{g}_k\|}{\sigma_k} - \frac{(1 - \eta_2)\epsilon}{12\sqrt{2}} \right], \quad (44)$$

for all $k \in \mathcal{U}$ sufficiently large. Because $\sqrt{\frac{\|\mathbf{g}_k\|}{\sigma_k}} \rightarrow 0$ as $k \rightarrow \infty$, the inequality (44) indicates $r_k < 0$ for all $k \in \mathcal{U}$ sufficiently large. Therefore, the k th iteration is very successful when $k \in \mathcal{U}$ is sufficiently large. Following from the updating procedure of σ_k in Algorithm 1, the inequality (36) holds. \square

According to the termination criteria in Algorithm 1, if the algorithm terminates finitely, then $\mathbf{g}(\mathbf{x}_*) = 0$ at the end point \mathbf{x}_* . Next we demonstrate that there exists a subsequence of $\{\mathbf{g}_k\}$ converging to zero when iteration points are infinite.

Theorem 4.1. *Suppose the infinite sequence $\{\mathbf{x}_k\}$ is produced by Algorithm 1. Then its gradient sequence $\{\mathbf{g}_k\}$ satisfies*

$$\liminf_{k \rightarrow \infty} \|\mathbf{g}_k\| = 0. \quad (45)$$

Proof. Assume $\|\mathbf{g}_k\| \geq \epsilon$. From (29) in Lemma 4.3, we have

$$\sigma_k \rightarrow +\infty,$$

which is incompatible with the conclusion

$$\sigma_{k+1} \leq \sigma_k, \quad \text{for sufficiently large } k$$

in Lemma 4.4. Therefore, the assumption is invalid and (45) holds. \square

Based on the conclusion in Theorem 4.1, we prove that the whole sequence $\{\mathbf{g}_k\}$ converges to zero.

Theorem 4.2. *Suppose the infinite sequence $\{\mathbf{x}_k\}$ is produced by Algorithm 1. Then its gradient sequence $\{\mathbf{g}_k\}$ satisfies*

$$\lim_{k \rightarrow \infty} \|\mathbf{g}_k\| = 0. \quad (46)$$

Proof. Assume (46) does not hold and there exists an infinite subsequence of iterations $\{t_i\}$ such that

$$\|\mathbf{g}_{t_i}\| \geq 2\epsilon, \quad \text{for some } \epsilon > 0 \text{ and for all } i. \quad (47)$$

On the other hand, Theorem 4.1 indicates that there is an infinite subsequence of $\{\mathbf{g}_k\}$ that converges to zero. Therefore, we choose the iteration sequence $\{l_i\}$ such that l_i is the first iteration satisfying

$$\|\mathbf{g}_{l_i}\| \leq \epsilon \quad (48)$$

after t_i , which means that for all i , we have

$$\|\mathbf{g}_m\| \geq \epsilon, \quad \text{for all } m \text{ with } t_i \leq m < l_i. \quad (49)$$

From (33), (34) and (35), we get

$$f(\mathbf{x}_m) - f(\mathbf{x}_{m+1}) \geq \frac{\alpha_{\min}^3 \eta_1 \epsilon}{36\sqrt{2}} \|\mathbf{p}_m\|, \quad \text{for all } t_i \leq m < l_i, \quad i \text{ sufficiently large.} \quad (50)$$

Summing up (50) from t_i to l_i-1 , we obtain

$$\begin{aligned} \frac{36\sqrt{2}}{\eta_1 \epsilon} [f(\mathbf{x}_{t_i}) - f(\mathbf{x}_{l_i})] &\geq \sum_{k=t_i}^{l_i-1} \alpha_{\min}^3 \|\mathbf{p}_k\| \\ &\geq \sum_{k=t_i}^{l_i-1} \alpha_{\min}^3 \|\mathbf{x}_{k+1} - \mathbf{x}_k\| \quad (\text{by (39)}) \\ &\geq \alpha_{\min}^3 \|\mathbf{x}_{t_i} - \mathbf{x}_{l_i}\| \end{aligned}$$

for all i sufficiently large.

In the proof process of Lemma 4.3, we have explained that the sequence $\{f(\mathbf{x}_k)\}$ is convergent. Thus $[f(\mathbf{x}_{t_i}) - f(\mathbf{x}_{l_i})] \rightarrow 0$ as $i \rightarrow +\infty$. Then the sequence $\|\mathbf{x}_{t_i} - \mathbf{x}_{l_i}\|$ converges to zero from the above inequalities. Since $\nabla^2 f(\mathbf{x})$ is bounded, $\mathbf{g}(\mathbf{x})$ is uniformly continuous, which implies that $\|\mathbf{g}_{t_i} - \mathbf{g}_{l_i}\|$ tends to zero as $\|\mathbf{x}_{t_i} - \mathbf{x}_{l_i}\|$ converges to zero. However, from (47) and (48) we have

$$\|\mathbf{g}_{t_i} - \mathbf{g}_{l_i}\| \geq \|\mathbf{g}_{t_i}\| - \|\mathbf{g}_{l_i}\| \geq \epsilon,$$

which produces a contradiction. Hence, the assumption (47) does not hold. The proof is completed. \square

5 Fast computation skill for $\mathcal{T}\mathbf{x}^{r-2}$

The eigenvalues of a symmetric tensor play an important role in spectral hypergraph theory. In the process of tensor eigenvalue computation, the operator $\mathcal{T}\mathbf{x}^{r-2}$ is frequently invoked. In this section, we introduce a fast computation skill FCS for tensor-vector product $\mathcal{T}\mathbf{x}^{r-2}$, in which the tensor \mathcal{T} is arisen from a hypergraph.

5.1 The basics of hypergraphs

Definition 5.1 (Hypergraph). *A hypergraph is defined as $G = (V, E)$, where $V = \{1, 2, \dots, n\}$ is the vertex set and $E = \{e_1, e_2, \dots, e_m\}$ is the edge set for $e_p \subset V, p = 1, 2, \dots, m$. If $|e_p| = r \geq 2$ for $p = 1, 2, \dots, m$ and $e_i \neq e_j$ when $i \neq j$, we call G an r -uniform hypergraph or an r -graph. If $r = 2$, G is an ordinary graph.*

For each vertex $i \in V$, the degree of i is defined as

$$d(i) = |\{e_p : i \in e_p, e_p \in E\}|.$$

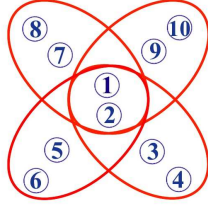


Figure 1: A 4-uniform flower hypergraph.

For instance, the flower hypergraph illustrated in Figure 1 is a 4-uniform hypergraph. There are ten vertices $V = \{1, 2, \dots, 10\}$ and four edges $E = \{e_1 = \{1, 2, 3, 4\}, e_2 = \{1, 2, 5, 6\}, e_3 = \{1, 2, 7, 8\}, e_4 = \{1, 2, 9, 10\}\}$ in this hypergraph. Its all edges share two common vertices, and the degree of each vertex is $d(1) = d(2) = 4$ and $d(i) = 1$ for $i = 3, 4, \dots, 10$.

Definition 5.2 (adjacency tensor [9]). *For an r -graph $G = (V, E)$ with n vertices, the adjacency tensor $\mathcal{A} = (a_{i_1 \dots i_r})$ of G is an r th order n -dimensional symmetric tensor with entries*

$$a_{i_1 \dots i_r} = \begin{cases} \frac{1}{(r-1)!} & \text{if } \{i_1, \dots, i_r\} \in E, \\ 0 & \text{otherwise.} \end{cases}$$

Definition 5.3 (Laplacian tensor and signless Laplacian tensor [23]). *For an r -graph $G = (V, E)$ with n vertices, the degree tensor \mathcal{D} is defined as an r th order n -dimensional diagonal tensor whose i th diagonal element is $d(i)$. Then the Laplacian tensor \mathcal{L} of G is defined as*

$$\mathcal{L} = \mathcal{D} - \mathcal{A},$$

and the signless Laplacian tensor \mathcal{Q} of G is defined as

$$\mathcal{Q} = \mathcal{D} + \mathcal{A}.$$

5.2 Calculation of $\mathcal{T}\mathbf{x}^{r-2}$

In order to compute the extreme Z-eigenvalue and H-eigenvalue of the adjacency tensor \mathcal{A} , the Laplacian tensor \mathcal{L} and the signless Laplacian tensor \mathcal{Q} , we need to compute products $\mathcal{T}\mathbf{x}^r$, $\mathcal{T}\mathbf{x}^{r-1}$ and $\mathcal{T}\mathbf{x}^{r-2}$ when $\mathcal{T} = \mathcal{A}$, \mathcal{L} and \mathcal{Q} . Chang et al. [4] provided an economical way to store a uniform hypergraph. Based on the economical storage, a fast method for computing products $\mathcal{T}\mathbf{x}^r$ and $\mathcal{T}\mathbf{x}^{r-1}$ was established. In this section, we introduce a fast tensor-vector product skill for $\mathcal{T}\mathbf{x}^{r-2}$, for $\mathcal{T} = \mathcal{A}$, \mathcal{L} and \mathcal{Q} .

Let $G = (V, E)$ be an r -uniform hypergraph with n vertices and m edges. We store G as an m -by- r matrix G_m whose each row represents an edge of G , and the entries in each row are vertices.

For example, we consider the 4-uniform flower hypergraph G which is shown in Figure 1. Then G can be stored by a 4-by-4 matrix

$$G_m = \begin{bmatrix} 1 & 2 & 3 & 4 \\ 1 & 2 & 5 & 6 \\ 1 & 2 & 7 & 8 \\ 1 & 2 & 9 & 10 \end{bmatrix} \in \mathbb{R}^{m \times r}. \quad (51)$$

Consider the degree tensor \mathcal{D} , whose i th diagonal element is the degree $d(i)$,

$$d(i) = \sum_{j=1}^r \sum_{l=1}^m \delta(i, (G_m)_{lj}), \quad \text{for } i = 1, 2, \dots, n.$$

Here $\delta(\cdot, \cdot)$ is the kronecker notation, i.e.

$$\delta(i, j) = \begin{cases} 1, & \text{if } i = j, \\ 0, & \text{if } i \neq j. \end{cases}$$

Then for any vector $\mathbf{x} \in \mathbb{R}^n$,

$$\mathcal{D}\mathbf{x}^{r-2} = \text{diag}\{d(1)x_1^{r-2}, \dots, d(n)x_n^{r-2}\}.$$

In order to compute $\mathcal{A}\mathbf{x}^{r-2}$, we construct another matrix $X_m = [x_{(G_m)_{lj}}]$ whose size is the same as that of G_m . If the (l, j) -th element of G_m is the vertex i , then the (l, j) -th element of X_m is x_i . For example, the matrix X_m corresponding to the matrix G_m in (51) is

$$X_m = \begin{bmatrix} x_1 & x_2 & x_3 & x_4 \\ x_1 & x_2 & x_5 & x_6 \\ x_1 & x_2 & x_7 & x_8 \\ x_1 & x_2 & x_9 & x_{10} \end{bmatrix}.$$

Based on the matrix X_m , we rewrite the calculation formula of $(\mathcal{A}\mathbf{x}^{r-2})_{ij}$ as

$$(\mathcal{A}\mathbf{x}^{r-2})_{ij} = \sum_{s=1}^m \sum_{\substack{l,k=1 \\ l \neq k}}^r \left(\delta(i, (G_m)_{sl}) \delta(j, (G_m)_{sk}) \prod_{\substack{t \neq l \\ t \neq k}} (X_m)_{st} \right), \quad \text{for } i, j = 1, 2, \dots, n.$$

We show the code for computing $\mathcal{T}\mathbf{x}^{r-2}$ in the figure 2.


```

1
2 % Store a 4-uniform flower hypergraph
3 Gm = [1,2,3,4; 1,2,5,6; 1,2,7,8; 1,2,9,10];
4
5 % Calculate the degree vector
6 [m,r] = size(Gm);
7 n      = max(Gm(:));
8 Md     = sparse(Gm(:),(1:m*r)',ones(m*r,1),n,m*r);
9 degree = full(sum(Md,2));
10
11 % Compute Dx^(r-2)
12 Dx2 = diag(degree.*(x.^(r-2)));
13
14 % Compute Ax^(r-2)
15 Xm  = reshape(x(Gm(:)),[m,k]);
16 Axk2 = zeros(n,n);
17 for i = 1:r-1
18     for j = i+1:r
19         A = Xm;
20         A(:,[i,j]) = [];
21         B = prod(A,2);
22         Axk2 = Axk2+sparse(Gm(:,i),Gm(:,j),B,n,n);
23     end
24 end
25 Axk2 = (Axk2+Axk2').*factorial(r-2)/factorial(r-1);
26
27 % Compute Lx^(r-2) and Qx^(r-2)
28 Lxk2 = Dxk2-Axk2;
29 Qxk2 = Dxk2+Axk2;

```

Figure 2: Code for computing $\mathcal{T}\mathbf{x}^{r-2}$

5.3 Test of the fast computation skill

In this section, we compare the fast computation skill FCS with the traditional algorithm for computing $\mathcal{A}\mathbf{x}^{r-2}$. Here \mathcal{A} refers to the adjacency tensor of the 4-uniform flower hypergraph in Figure 1. In Tensor Toolbox, the traditional algorithm for computing $\mathcal{A}\mathbf{x}^{r-2}$ is implemented as `ttsv`. The vector $\mathbf{x} \in \mathbb{R}^n$ is randomly generated. All numerical experiments in this paper are carried by a laptop with i5-10210U CPU at 1.60GHz and 16.0GB of RAM .

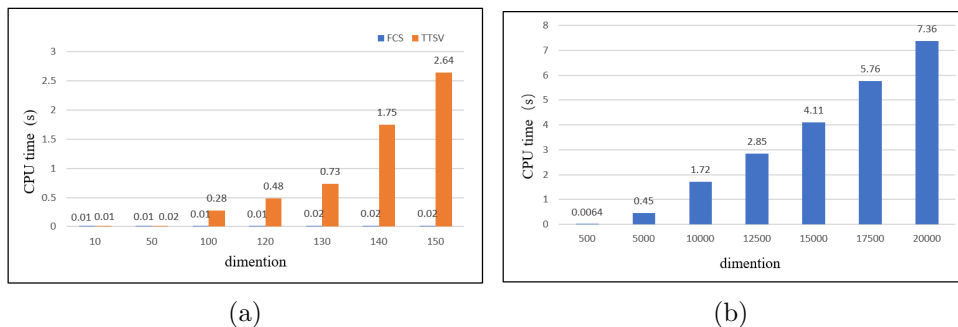


Figure 3: CPU time for computing $\mathcal{A}\mathbf{x}^{r-2}$ with different dimensions n .

The performance of computing $\mathcal{A}\mathbf{x}^{r-2}$ by FCS and `ttsv` are shown in Figure 3. As shown in Figure 3 (a), when $n \leq 150$, it takes about 0.01s for FCS to calculate $\mathcal{A}\mathbf{x}^{r-2}$. With the increase of the dimension n , `ttsv` spends much more time to calculate $\mathcal{A}\mathbf{x}^{r-2}$ than time taken by FCS. Furthermore, our laptop is incapable of computing eigenvalues of tensors with dimension greater than 150 by `ttsv`, while FCS can compute tensors of higher dimensions. Figure 3 (b) demonstrates the results of CPU time for calculating $\mathcal{A}\mathbf{x}^{r-2}$ with large n by FCS. Up to 20000 dimensions, the calculation by FCS costs less than 8 seconds.

6 Numerical experiments

In order to show the efficiency of the proposed adaptive cubic regularization algorithm (ACRCET), we perform some numerical experiments. In this section, three other algorithms are compared with ACRCET .

- An adaptive power method (PM) [14, 15]. In Tensor Toolbox, it is implemented as `eig_sshopm` and `eig_geap` for Z-eigenvalues and H-eigenvalues of even order symmetric tensors, respectively.
- A curvilinear search algorithm (ACSA) [8] which employs the Barzilai-Borwein gradient optimization algorithm for computing tensor eigenvalues. The code was provided by the authors of [8].
- An unconstrained optimization approach (HUOA) [12]. The author employs the local optimization solver `fminunc` from the Optimization Toolbox to solve an unconstrained optimization model.

The ACRCET algorithm is implemented with following parameters

$$\eta_1 = 0.1, \eta_2 = 0.5, \gamma_1 = 0.25, \gamma_2 = 1.2, \text{ and } \gamma_3 = 2.$$

We solve the subproblem based on the method given in [1, Section 6]. First we employ the Lanczos method to simplify the subproblem (12) as

$$m(\mathbf{u}) = f_k + \gamma \mathbf{u}^T \mathbf{e}_1 + \frac{1}{2} \mathbf{u}^T T_k \mathbf{u} + \frac{1}{3} \sigma_k \|\mathbf{u}\|^3,$$

where \mathbf{e}_1 is a unit vector and T is a symmetric tridiagonal matrix. Similar to the trust region method, it is proved in [1, Theorem 3.1] that \mathbf{u} is a global minimizer of the above subproblem if and only if a pair of (\mathbf{u}, λ) satisfies

$$(T_k + \lambda I)\mathbf{u} = -\gamma \mathbf{e}_1 \text{ and } \lambda^2 = \sigma_k^2 \mathbf{u}^T \mathbf{u} \quad (52)$$

where $T_k + \lambda I$ is positive semidefinite. The equation system (52) is finally solved by Newton's method [1, Algorithm 6.1].

We compute the extreme H- or Z-eigenvalue of a tensor by running four algorithms PM, ACSA, HUOA, and ACRCET from 100 random initial points sampled on the unit sphere \mathbb{S}^{n-1} . Then we obtain 100 estimated eigenvalues and take the best one as the estimated extreme eigenvalue. In the following experiments, we report the estimated extreme eigenvalue, the total number of iterations (Iter'n) and the total CPU time (Time in seconds) of the 100 runs.

Example 1 In [22], Qi generated a symmetric tensor $\mathcal{A}(\alpha) \in \mathbb{R}^{[4,2]}$ with

$$a_{1111} = 3, a_{2222} = 1, a_{1122} = a_{1221} = a_{1212} = a_{2121} = a_{2211} = a_{2112} = \alpha$$

and other entries being zero. For different values of α , all Z-eigenvalues of $\mathcal{A}(\alpha)$ are analyzed and provided in [22]. Thus we know the smallest Z-eigenvalue of $\mathcal{A}(\alpha)$ for $\alpha = 0, 10$ and 100 are

$$\lambda_{\min}^Z(\mathcal{A}(0)) = \frac{3}{4}, \lambda_{\min}^Z(\mathcal{A}(10)) = \lambda_{\min}^Z(\mathcal{A}(100)) = 1.$$

We compute the smallest Z-eigenvalues of $\mathcal{A}(\alpha)$ when $\alpha = 0, 10$ and 100 by PM, ACSA, HUOA and ACRCET. The numerical results are shown in Table 1. It can be seen that both PM and ACRCET find all the true smallest eigenvalues. When $\alpha = 10$ or 100, ACSA gives one of the Z-eigenvalues of $\mathcal{A}(\alpha)$, but misses the smallest one. When $\alpha = 0$ or 10, HUOA obtains the smallest Z-eigenvalue of $\mathcal{A}(\alpha)$ inaccurately. Since second order information from the Hessian and cubic overestimator of the objective function are employed, the proposed ACRCET performs much better than other algorithms.

Example 2 (A 2-Regular Hypergraph). A regular hypergraph is a hypergraph whose vertices have the same degree. For the hypergraph presented in Figure 4, the degree of all its vertices is 2. We call it a 2-regular hypergraph and denote it as G_R^2 . Define the H-spectral radius of a tensor \mathcal{T} as the largest modulus of the H-eigenvalues of \mathcal{T} , and we use $\rho(\mathcal{T})$ to stand for the H-spectral radius of \mathcal{T} .

Table 1: Results for finding the smallest Z-eigenvalues of Example 1.

Algorithms	$\alpha = 0$			$\alpha = 10$			$\alpha = 100$		
	λ_{\min}^Z	Iter'n	Time(s)	λ_{\min}^Z	Iter'n	Time(s)	λ_{\min}^Z	Iter'n	Time(s)
PM	0.7500	813	0.26	1.0000	588	0.21	1.0000	561	0.29
ACSA	0.7500	800	0.11	3.0000(*)	500	0.12	3.0000(*)	500	0.10
HUOA	0.7533(*)	3219	1.34	1.1149(*)	2893	1.33	1.0000	3219	1.47
ACRCET	0.7500	200	0.12	1.0000	200	0.13	1.0000	400	0.15

Table 2: Results for finding the largest H-eigenvalue of $\mathcal{Q}(G_R^2)$ and the smallest H-eigenvalue of $\mathcal{A}(G_R^2)$.

Algorithms	$\lambda_{\max}^H(\mathcal{Q}(G_R^2))$	Iter'n	Time(s)	$\lambda_{\min}^H(\mathcal{A}(G_R^2))$	Iter'n	Time(s)
PM	4.0000	4310	2.52	-2.0000	4596	3.06
ACSA	4.0000	2952	1.97	-2.0000	2876	2.05
HUOA	4.0000	3304	1.82	-2.0000	3297	1.63
ACRCET	4.0000	616	0.71	-2.0000	618	0.60

Proposition 6.1 ([24]). *Suppose G is a d -regular hypergraph. The H -spectral radius of its signless Laplacian tensor $\rho(\mathcal{Q}(G)) = 2d$ and the H -spectral radius of its adjacency tensor $\rho(\mathcal{A}(G)) = d$.*

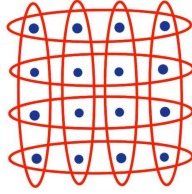


Figure 4: A 4-uniform 2-regular hypergraph.

We compute the largest H-eigenvalue of the signless Laplacian tensor $\mathcal{Q}(G_R^2)$ and the smallest H-eigenvalue of the adjacency tensor $\mathcal{A}(G_R^2)$. The results are shown in Table 2. From Proposition 6.1, we know $\rho(\mathcal{Q}(G_R^2)) = 4$ and $\rho(\mathcal{A}(G_R^2)) = 2$. The extreme eigenvalues calculated by PM, ACSA, HUOA, and ACRCET agree with this conclusion. It can be seen that ACRCET runs much faster than the other three methods.

Example 3 (Loose Cycle). For a k -uniform hypergraph, if its vertex set $V = \{i_{1,1}, \dots, i_{1,k-1}, i_{2,1}, \dots, i_{2,k-1}, \dots, i_{k,1}, \dots, i_{k,k-1}\}$ and its edge set $E = \{(i_{1,1}, \dots, i_{1,k-1}, i_{2,1}), (i_{2,1}, \dots, i_{2,k-1}, i_{3,1}), \dots, (i_{k,1}, \dots, i_{k,k-1}, i_{1,1})\}$, then it is called a loose cycle. We denote the k -uniform loose cycles with m edges as $G_L^{k,m}$. Given a graph G , if we add $k - 2$ different vertices in its each edge, then we get its k th power hypergraph G^k . For example, the 4-uniform loose cycles $G_L^{4,3}$ and $G_L^{4,6}$ in Figure 5 (c) and (d) are the 4th power hypergraph of the graphs $G_L^{2,3}$ and $G_L^{2,6}$ in Figure 5 (a) and (b) respectively. We list some conclusions about

spectral radius of loose cycles and power hypergraphs below.

Proposition 6.2 ([24]). *If the spectral radius of the adjacency matrix of a graph G is $\rho(A(G))$, then the H-spectral radius of the adjacency tensor of its k th power hypergraph $\rho(\mathcal{A}(G^k)) = \rho(A(G))^{\frac{2}{k}}$.*

Since 2-uniform loose cycles $G_L^{2,m}$ are 2-regular, we obtain $\rho(A(G_L^{2,m})) = 2$ from Proposition 6.1. Therefore, based on Proposition 6.2, the H-spectral radius of the adjacency tensor of the 4th power hypergraph $G_L^{4,m}$ of $G_L^{2,m}$

$$\rho(\mathcal{A}(G_L^{4,m})) = \rho(A(G_L^{2,m}))^{\frac{2}{4}} = \sqrt{2}, \text{ for } m = 3, 4, 5, \dots \quad (53)$$

Proposition 6.3 ([27], [13]). *For a d -regular graph G , the H-spectral radius of the signless Laplacian tensor of its k th power hypergraph $\rho(\mathcal{Q}(G^k))$ is the root of the equation*

$$(x - d)(x - 1)^{\frac{k-2}{2}} - d = 0. \quad (54)$$

If k is even, then for any graph, the H-spectral radii of the signless Laplacian tensor and Laplacian tensor of its k th power hypergraph are equal. That is $\rho(\mathcal{Q}(G^k)) = \rho(\mathcal{L}(G^k))$.

When $k = 4, d = 2$ the root of equation (54) is 3. Thus from Proposition 6.3, the H-spectral radius of the signless Laplacian tensor and Laplacian tensor of $G_L^{4,m}$

$$\rho(\mathcal{Q}(G_L^{4,m})) = \rho(\mathcal{L}(G_L^{4,m})) = 3, \text{ for } m = 3, 4, 5, \dots \quad (55)$$

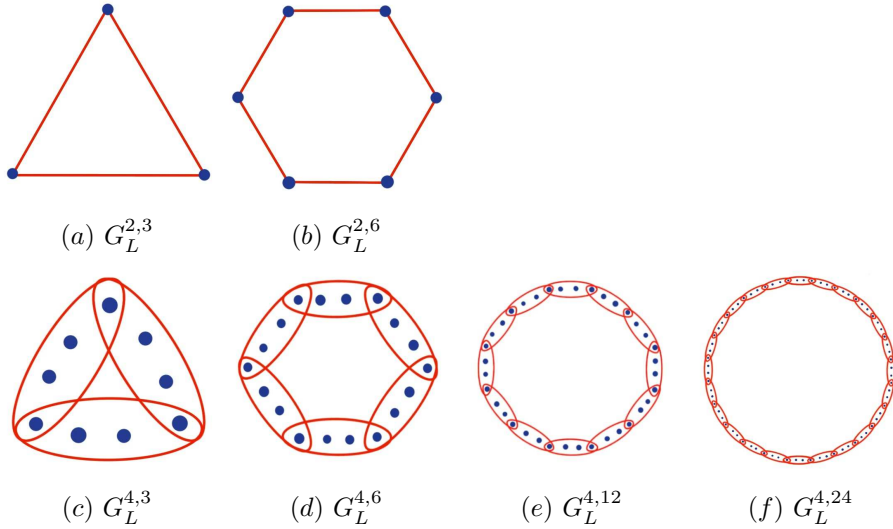


Figure 5: 2-uniform loose cycles, the corresponding 4th power hypergraphs and other 4-uniform loose cycles.

Table 3: Results for finding the largest H-eigenvalues of $\mathcal{A}(G_L^{4,m})$ and $\mathcal{L}(G_L^{4,m})$.

	Algorithms	$\lambda_{\max}^H(\mathcal{A}(G_L^{4,m}))$	Iter'n	Time(s)	$\lambda_{\max}^H(\mathcal{L}(G_L^{4,m}))$	Iter'n	Time(s)
$m = 3$	PM	1.4142	4894	1.34	3.0000	4082	1.45
	ACSA	1.4142	2494	1.33	3.0000	3065	1.49
	HUOA	1.4142	2654	1.79	3.0000	2740	1.84
	ACRCET	1.4142	532	0.47	3.0000	598	0.68
$m = 6$	PM	1.4142	14937	5.91	3.0000	13158	5.48
	ACSA	1.4142	8628	5.09	3.0000	8634	4.99
	HUOA	1.4142	4621	2.91	3.0000	5094	3.01
	ACRCET	1.4142	808	0.92	3.0000	983	1.19
$m = 12$	PM	1.4142	48724	106.34	3.0000	46426	102.99
	ACSA	1.4142	18581	71.07	3.0000	16325	62.78
	HUOA	1.4142	8956	12.08	3.0000	10711	13.14
	ACRCET	1.4142	1343	1.83	3.0000	1857	2.69

Table 4: Performance of ACRCET for finding the largest Z-eigenvalues of $\mathcal{Q}(G_L^{4,m})$.

n	m	$\lambda_{\max}^Z(\mathcal{Q}(G_L^{4,m}))$	Iter'n	Time(s)
9	3	2	350	0.42
18	6	2	340	0.69
36	12	2	635	1.10
72	24	2	586	1.76
144	48	2	598	4.20
288	96	2	690	15.06
576	192	2	665	147.40
1152	384	2	728	1020.07
2304	768	2	811	9745.41

We compute the largest H-eigenvalues of adjacency tensors $\mathcal{A}(G_L^{4,m})$ and Laplacian tensors $\mathcal{L}(G_L^{4,m})$ of the 4-uniform loose cycles in Figure 5 (c), (d) and (e) when $m = 3, 6, 12$. Table 3 reports the results calculated by PM, ACSA, HUOA and ACRCET. Obviously, the H-eigenvalues of $\mathcal{A}(G_L^{4,m})$ and $\mathcal{L}(G_L^{4,m})$ given by these four methods coincide with the theoretical results in (53) and (55). Compared with PM, ACSA and HUOA, ACRCET saves more than a half iterations and costs much less time. Because of the memory limitation of our laptop, PM, ACSA and HUOA are executable only under the condition $m \leq 48$.

We show the performance of ACRCET for computing the largest Z-eigenvalues of signless Laplacian tensors $\mathcal{Q}(G_L^{4,m})$ of 4-uniform loose cycles for different m in Table 4. It can be seen that the ACRCET method is able to compute the largest Z-eigenvalues of tensors with dimensions n up to more than two thousands. Although the relationship between the Z-spectral radius of a graph and the Z-spectral radius of its power hypergraph is not clear, it seems from the numerical results that a result about Z-spectral radius similar to the conclusion in Proposition 6.2 holds for 4th power hypergraph of 2-uniform loose cycles.

7 Conclusion

In this paper we have used the adaptive cubic regularization method to compute extreme H- and Z-eigenvalues of even order symmetric tensors. We have established a fast computing skill, which has been proven effective in our test, for the matrix-valued products $\mathcal{T}\mathbf{x}^{r-2}$ of a vector \mathbf{x} and a tensor \mathcal{T} arising from a uniform hypergraph. Numerical experiments show that our ACR CET algorithm performs well for even order symmetric tensor problems. Our next goal is to further study the cubic regularization method for constrained optimization problems, and improve the computation efficiency of the cubic subproblem so that large scale problems can be calculated efficiently.

References

- [1] Coralia Cartis, Nicholas IM Gould, and Philippe L Toint. Adaptive cubic regularisation methods for unconstrained optimization. part i: motivation, convergence and numerical results. *Mathematical Programming*, 127(2):245–295, 2011.
- [2] Coralia Cartis, Nicholas IM Gould, and Philippe L Toint. Adaptive cubic regularisation methods for unconstrained optimization. part ii: worst-case function-and derivative-evaluation complexity. *Mathematical programming*, 130(2):295–319, 2011.
- [3] Arthur Cayley. About the algebraic structure of the orthogonal group and the other classical groups in a field of characteristic zero or a prime characteristic. *Reine Angewandte Mathematik*, 32(1846):6, 1846.
- [4] Jingya Chang, Yannan Chen, and Liqun Qi. Computing eigenvalues of large scale sparse tensors arising from a hypergraph. *SIAM Journal on Scientific Computing*, 38(6):A3618–A3643, 2016.
- [5] Liping Chen, Lixing Han, Hongxia Yin, and Liangmin Zhou. A homotopy method for computing the largest eigenvalue of an irreducible nonnegative tensor. *Journal of Computational and Applied Mathematics*, 355:174–181, 2019.
- [6] Liping Chen, Lixing Han, and Liangmin Zhou. Computing tensor eigenvalues via homotopy methods. *SIAM Journal on Matrix Analysis and Applications*, 37(1):290–319, 2016.
- [7] Yannan Chen, Yuhong Dai, Deren Han, and Wenyu Sun. Positive semidefinite generalized diffusion tensor imaging via quadratic semidefinite programming. *SIAM Journal on Imaging Sciences*, 6(3):1531–1552, 2013.
- [8] Yannan Chen, Liqun Qi, and Qun Wang. Computing extreme eigenvalues of large scale Hankel tensors. *Journal of scientific computing*, 68(2):716–738, 2016.

- [9] Joshua Cooper and Aaron Dutle. Spectra of uniform hypergraphs. *Linear Algebra and its applications*, 436(9):3268–3292, 2012.
- [10] Chunfeng Cui, Yuhong Dai, and Jiawang Nie. All real eigenvalues of symmetric tensors. *SIAM Journal on Matrix Analysis and Applications*, 35(4):1582–1601, 2014.
- [11] Andreas Griewank. The modification of newton’s method for unconstrained optimization by bounding cubic terms. Technical report, Technical report NA/12, 1981.
- [12] Lixing Han. An unconstrained optimization approach for finding real eigenvalues of even order symmetric tensors. *Numerical Algebra, Control and Optimization*, 3(3):583, 2013.
- [13] Shenglong Hu, Liqun Qi, and Jiayu Shao. Cored hypergraphs, power hypergraphs and their laplacian H-eigenvalues. *Linear Algebra and Its Applications*, 439(10):2980–2998, 2013.
- [14] Tamara G Kolda and Jackson R Mayo. Shifted power method for computing tensor eigenpairs. *SIAM Journal on Matrix Analysis and Applications*, 32(4):1095–1124, 2011.
- [15] Tamara G Kolda and Jackson R Mayo. An adaptive shifted power method for computing generalized tensor eigenpairs. *SIAM Journal on Matrix Analysis and Applications*, 35(4):1563–1581, 2014.
- [16] Yueh-Cheng Kuo, Wen-Wei Lin, and Ching-Sung Liu. Continuation methods for computing Z-/H-eigenpairs of nonnegative tensors. *Journal of Computational and Applied Mathematics*, 340:71–88, 2018.
- [17] Guoyin Li, Liqun Qi, and Gaohang Yu. The Z-eigenvalues of a symmetric tensor and its application to spectral hypergraph theory. *Numerical Linear Algebra with Applications*, 20(6):1001–1029, 2013.
- [18] Wen Li and Michael K Ng. On the limiting probability distribution of a transition probability tensor. *Linear and Multilinear Algebra*, 62(3):362–385, 2014.
- [19] Lek-Heng Lim. Singular values and eigenvalues of tensors: a variational approach. In *1st IEEE International Workshop on Computational Advances in Multi-Sensor Adaptive Processing*, pages 129–132. IEEE, 2005.
- [20] Yurii Nesterov and Boris T Polyak. Cubic regularization of Newton method and its global performance. *Mathematical Programming*, 108(1):177–205, 2006.
- [21] Michael Ng, Liqun Qi, and Guanglu Zhou. Finding the largest eigenvalue of a nonnegative tensor. *SIAM Journal on Matrix Analysis and Applications*, 31(3):1090–1099, 2010.

- [22] Liqun Qi. Eigenvalues of a real supersymmetric tensor. *Journal of Symbolic Computation*, 40(6):1302–1324, 2005.
- [23] Liqun Qi. H^+ -eigenvalues of laplacian and signless laplacian tensors. *Communications in mathematical sciences*, 12(6):1045–1064, 2013.
- [24] Liqun Qi and Ziyang Luo. *Tensor analysis: spectral theory and special tensors*. SIAM, 2017.
- [25] Zhou Sheng and Qin Ni. Computing tensor Z -eigenvalues via shifted inverse power method. *Journal of Computational and Applied Mathematics*, 398:113717, 2021.
- [26] Peng Xu, Fred Roosta, and Michael W Mahoney. Newton-type methods for non-convex optimization under inexact hessian information. *Mathematical Programming*, 184(1):35–70, 2020.
- [27] Jiang Zhou, Lizhu Sun, Wenzhe Wang, and Changjiang Bu. Some spectral properties of uniform hypergraphs. *The Electronic Journal of Combinatorics*, 21(4):p4.24, 2014.